*Am J Physiol Heart Circ Physiol* 311: H1287–H1296, 2016.
First published August 5, 2016; doi:10.1152/ajpheart.00096.2016.

# Cardiac-deleterious role of galectin-3 in chronic angiotensin II-induced hypertension

**Germán E. González,[1,3]* N.-E. Rhaleb,[1,4]* Martin A. D'Ambrosio,[1] Pablo Nakagawa,[1] Tang-Dong Liao,[1] Edward L. Peterson,[2] Pablo Leung,[1] Xiangguo Dai,[1] Branislava Janic,[1] Yun-He Liu,[1] Xiao-Ping Yang,[1] and Oscar A. Carretero[1]**

[1]*Hypertension and Vascular Research Division, Department of Internal Medicine, Henry Ford Hospital, Detroit, Michigan;* [2]*Department of Public Health Sciences, Henry Ford Hospital, Detroit, Michigan;* [3]*Cardiovascular Pathophysiology Institute, Department of Pathology, University of Buenos Aires, Buenos Aires, Argentina; and* [4]*Department of Physiology, Wayne State University, Detroit, Michigan*

Submitted 29 January 2016; accepted in final form 3 August 2016

**González GE, Rhaleb N, D'Ambrosio MA, Nakagawa P, Liao T, Peterson EL, Leung P, Dai X, Janic B, Liu Y, Yang X, Carretero OA.** Cardiac-deleterious role of galectin-3 in chronic angiotensin II-induced hypertension. *Am J Physiol Heart Circ Physiol* 311: H1287–H1296, 2016. First published August 5, 2016; doi:10.1152/ajpheart.00096.2016.—Galectin-3 (Gal-3), a member of the β-galactoside lectin family, has an important role in immune regulation. In hypertensive rats and heart failure patients, Gal-3 is considered a marker for an unfavorable prognosis. Nevertheless, the role and mechanism of Gal-3 action in hypertension-induced target organ damage are unknown. We hypothesized that, in angiotensin II (ANG II)-induced hypertension, genetic deletion of Gal-3 prevents left ventricular (LV) adverse remodeling and LV dysfunction by reducing the innate immune responses and myocardial fibrosis. To induce hypertension, male C57BL/6J and Gal-3 knockout (KO) mice were infused with ANG II (3 $\mu g \cdot min^{-1} \cdot kg^{-1}$ sc) for 8 wk. We assessed: *1*) systolic blood pressure by plethysmography, *2*) LV function and remodeling by echocardiography, *3*) myocardial fibrosis by histology, *4*) cardiac $CD68^+$ macrophage infiltration by histology, *5*) ICAM-1 and VCAM-1 expression by Western blotting, *6*) plasma cytokines, including interleukin-6 (IL-6), by enzyme-linked immunosorbent assay, and *7*) regulatory T ($T_{reg}$) cells by flow cytometry as detected by their combined expression of CD4, CD25, and FOXP3. Systolic blood pressure and cardiac hypertrophy increased similarly in both mouse strains when infused with ANG II. However, hypertensive C57BL/6J mice suffered impaired ejection and shortening fractions. In these mice, the extent of myocardial fibrosis and macrophage infiltration was greater in histological sections, and cardiac ICAM-1, as well as plasma IL-6, expression was higher as assessed by Western blotting. However, all these parameters were blunted in Gal-3 KO mice. Hypertensive Gal-3 KO mice also had a higher number of splenic $T_{reg}$ lymphocytes. In conclusion, in ANG II-induced hypertension, genetic deletion of Gal-3 prevented LV dysfunction without affecting blood pressure or LV hypertrophy. This study indicates that the ANG II effects are, in part, mediated or triggered by Gal-3 together with the related intercellular signaling (ICAM-1 and IL-6), leading to cardiac inflammation and fibrosis.

angiotensin II; hypertension; inflammation; galectin-3; interleukin-6; fibrosis; macrophages

**NEW & NOTEWORTHY**

*Our study suggests that galectin-3 should be considered not merely a marker for heart failure, but also a direct mediator of cardiac inflammation, fibrosis, and dysfunction. Thus, antagonistic strategies targeting galectin-3 may be a novel therapeutic approach in providing cardiac protection in hypertension and heart failure.*

GALECTINS ARE SOLUBLE LECTINS with intra- and extracellular functions. Extracellularly, secreted galectins modulate immunity and inflammation by binding a preferred set of cell surface glycol conjugates, such as membrane glycolipids and transmembrane glycoproteins (38).

Galectin-3 (Gal-3) is a ~30-kDa β-galactoside-binding protein predominantly and widely expressed in the immune system. Previous findings indicate that Gal-3 is differentially expressed in various mouse organs (22). Macrophages and fibroblasts have been considered the main source of Gal-3 (10). This immunomodulatory lectin regulates apoptosis, as well as cell proliferation and growth, likely by orchestrating cell-cell and cell-extracellular matrix interactions. However, Gal-3 has a stimulatory effect on inflammation and components of innate immunity. For example, Gal-3 stimulates production of proinflammatory mediators and reactive oxygen species in mast cells, neutrophils, and macrophages (8), and these cells migrate to and infiltrate the sites of injury by binding to adhesion molecules such as ICAM-1 and VCAM-1 on endothelial cells. In an experimental model of cardiac disease, Gal-3 was shown to be expressed in inflammatory cells infiltrating the heart; Gal-3 also induced fibroblast proliferation, cyclin D1 expression, and collagen production by cardiac fibroblasts (43). In hypertensive rats and patients with heart failure, Gal-3 is a marker for poor prognosis (30, 43). Additionally, Gal-3 is a pathogenic factor in heart failure, because we have shown that infusion of exogenous Gal-3 into the pericardial sac causes myocardial inflammation and fibrosis and also impairs left ventricular (LV) contractility without affecting blood pressure (26), whereas Yu et al. (51) showed that Gal-3 actively contributed to cardiac remodeling, myocardial fibrogenesis, and heart failure. Furthermore, we recently showed that genetic deletion of Gal-3 reduced myocardial macrophage infiltration and fibrosis during the healing phase in myocardial infarction in mice (14). Furthermore, myocardial hypertrophy and ventricular dysfunction induced by aortic constriction or angiotensin II (ANG II) were blunted in Gal-3 knockout (KO) mice, as well as in mice with pharmacological inhibition of Gal-3 (51). However, the role of Gal-3 in chronic hypertensive

* G. E. González and N.-E. Rhaleb contributed equally to this work.

Address for reprint requests and other correspondence: O. A. Carretero, Hypertension and Vascular Research Division, Dept. of Internal Medicine, Henry Ford Hospital, 2799 West Grand Blvd., Detroit, MI 48202 (e-mail: ocarret1@hfhs.org).

  

heart remodeling and cardiac inflammation and dysfunction is far from being elucidated.

Galectins, including Gal-3, are known for their negative effects on T cell proliferation and survival. Previous studies showed that Gal-3 deficiency increases the peripheral regulatory T ($T_{reg}$) cell frequency in leshmaniasis (13) and in mouse experimental autoimmune myocarditis (21), indicating that, under pathological conditions, Gal-3 regulates T cells. However, the role of Gal-3 in $T_{reg}$ cells during hypertension has not been examined. Therefore, we hypothesize that, in chronic ANG II-induced hypertension, Gal-3 decreases the number of $T_{reg}$ lymphocytes by increasing circulating inflammatory cytokine concentrations and adhesion molecule expression, thus contributing to cardiac inflammation, fibrosis, and dysfunction. To dissect the role of Gal-3 in ANG II-induced hypertension, as well as cardiac remodeling and function, we infused ANG II or its vehicle into Gal-3 KO mice and their wild-type counterparts and then analyzed plasma proinflammatory cytokine concentrations, adhesion molecule expression, and circulating lymphocyte populations.

## METHODS

### *Mice and Experimental Design*

We used male C57BL/6J and Gal-3 KO mice (13–15 wk old). C57BL/6J mice (Jackson Laboratories) were used as controls. Gal-3 KO mice, originally developed by Hsu et al. (20), were bred on a C57BL/6J background at the Henry Ford Hospital bioresources facilities. Mice were anesthetized with pentobarbital sodium (50 mg/kg ip), and osmotic minipumps (Alzet 2004, Durect, Cupertino, CA) were implanted subcutaneously under aseptic conditions, as previously described (37), to deliver ANG II (3 $\mu g \cdot min^{-1} \cdot kg^{-1}$) (4, 15) or its vehicle (0.01 N acetic acid) (15). Mice were divided into four experimental groups as follows: *1*) C57BL/6J vehicle, *2*) Gal-3 KO vehicle, *3*) C57BL/6J ANG II, and *4*) Gal-3 KO. Treatment continued for 8 wk. This protocol was approved by the Henry Ford Hospital Institutional Animal Care and Use Committee and followed the National Institutes of Health *Guide for the Care and Use of Laboratory Animals*.

### *Systolic Blood Pressure*

A noninvasive computerized tail-cuff system (model BP-2000, Visitech, Apex, NC) was used to measure systolic blood pressure (SBP) in conscious mice at baseline and then three times weekly. Each SBP consisted of 3 sets of 10 measurements, with each set of 10 measurements including >6 successful measurements. Weekly SBP readings were averaged, as previously described (45).

### *Echocardiography*

*Echocardiographic recording.* Before beginning the studies, the mice were trained as follows. The animals were picked up by the nape of the neck and held firmly in the palm of the examiner's hand in the supine position with the tail held tightly between the last two fingers. The left hemithorax was carefully shaved, and prewarmed ultrasound transmission gel (Parker Laboratory, Orange, NJ) was applied. The transducer probe was gently applied to the left chest, and images obtained during the training sessions were not recorded. We previously reported that, with repeated training, mice remain calm and their heart rate stabilizes at 600–700 beats/min, which is comparable to the heart rate of conscious mice subjected to the tail-cuff or telemetry method (15, 50). After the mice were well trained, transthoracic echocardiographic studies were performed using an ultrasound machine (model 256, Acuson) equipped with a 15-MHz linear transducer (model 15L8, Acuson). Generally, the heart was first imaged in the two-dimensional (2-D) mode in the parasternal long-axis view. From this view, an M-mode cursor was positioned perpendicular to the interventricular septum and posterior wall of the LV at the level of the papillary muscles, and M-mode images were obtained for measurement of wall thickness and chamber dimensions. Then a 2-D short-axis view of the mid-LV was obtained at the chordal level. Images from this view were used to measure LV chamber area. Images were stored in digital format on a magnetic optical disk for review and analysis.

*Image analysis.* LV end-diastolic dimension (LVDd), end-systolic dimension (LVDs), interventricular septum thickness (IVST), and posterior wall thickness (PWT) were measured from the M-mode traces. During diastole, LV dimension and wall thickness were measured from the maximum chamber cavity; during systole, the same parameters were measured during the maximum anterior motion of the posterior wall, according to the American Society of Echocardiography guidelines (40). Shortening fraction (SF), a measure of LV systolic function, was calculated from the M-mode LV internal dimensions using the following equation: SF (%) = [(LVDd − LVDs)/LVDd] × 100. Ejection fraction (EF) was calculated from the LV cross-sectional area (2-D short-axis view) using the following equation: EF (%) = [(LVAd − LVAs)/LVAd] × 100, where LVAd is LV diastolic area and LVAs is LV systolic area. All primary measurements, such as LV wall thickness, dimensions, and cross-sectional areas, were traced manually and digitized by goal-directed, diagnostically driven software installed on the echocardiograph. Three beats were averaged for each measurement.

### *Organ Harvest*

At the end of the protocol, animals were anesthetized with pentobarbital sodium (50 mg/kg ip), and blood was collected for cytokine analysis. The heart was stopped at diastole by 15% KCl injection, then the heart, lung, and spleen were rapidly excised. The lungs and the LV (including the septum) were weighed, and the LV was sectioned transversely into two slices. A pool of LVs were embedded in Tissue-Tek OCT (Sakura Finetek, Torrance, CA), dipped in isopentane that was precooled in liquid nitrogen for rapid freezing, and stored at −70°C until further processing. Tissue slices were later cut into 6-μm-thick sections and then analyzed by histopathology and immunohistochemistry (29). The other pool of LVs was saved in a dry tube and snap-frozen in liquid nitrogen for Western blot analysis (25). The right limb was excised, and the tibia length (TL) was measured to normalize heart weight and LV weight.

### *Histopathological Studies*

Frozen sections were double-stained with fluorescein-labeled peanut agglutinin [to outline the myocyte cross-sectional area (MCSA) and the interstitial space] and rhodamine-labeled *Griffonia simplicifolia* lectin I [to outline the microvessels such as small arteries (20 μm), normal capillaries (3–6 μm), and venous capillaries (6–9 μm)] (17, 18, 39). This labeling allows identification of both myocytes and capillaries, as previously described (49). Radially oriented microscopic fields from each section were photographed at ×400 magnification on a microscope (model IX81, Olympus America, Center Valley, PA) equipped with a digital camera (model DP70, Olympus America) and analyzed with a computerized image analysis system (MicroSuite Biological, Olympus America). MCSA was measured by computer-based planimetry in 140–240 myocytes per animal, and data obtained from the same tissue of the same animal were averaged. Capillary density is expressed as the number of capillaries per square millimeter of myocardial area (49). Additional slices were stained with PicroSirius red to determine myocardial fibrosis. The collagen volume fraction was assessed by an operator blind to the samples in 10–35 (mean 17.6) random images and calculated as the ratio of the collagen area to the entire area of an individual section, which is the

sum of the areas representing the myocyte and interstitial space (18, 29, 39).

*Immunohistochemistry*

Frozen sections were immunostained with anti-rat CD68 antibody (specific for a macrophage marker, 1:200 dilution; AbD Serotec, Raleigh, NC) and then incubated with a horse anti-mouse biotinylated secondary antibody (1:200 dilution; AbD Serotec). Vectastain Elite avidin-biotin complex-peroxidase kits (Vector Laboratories, Burlingame, CA) and 3-amino-9-ethylcarbazole substrate (Life Technologies, Grand Island, NY) were used to detect signals. Negative controls were processed in the same fashion, except for the step where the primary antibody was omitted. Positive cells (reddish-brown staining) were counted at ×400 magnification in 10–15 randomly chosen fields per section and expressed as number of cells per square millimeter.

*Cytokine Measurements With Cytometric Bead Array*

Six inflammatory cytokines and a chemokine [IL-6, IL-10, IFN-γ, monocyte chemoattractant protein-1 (MCP-1), IL-10, IL-12, and TNF-α] were analyzed using cytometric bead array (Mouse Inflammation Kit, BD Biosciences, San Jose, CA) according to the manufacturer's protocol. Cytokine concentrations are expressed as picograms per milliliter of plasma.

*Western Blotting*

Cardiac ICAM-1 and VCAM-1 expression was measured by Western blotting. Briefly, ~25 mg of LV tissue were homogenized in 300 μl of CelLytic (Sigma Aldrich, St. Louis, MO) on ice and centrifuged at 4,000 *g* for 10 min. Protein (10 μg) from the LV extracts was loaded onto a 10% SDS-polyacrylamide gel under nonreducing conditions, electrophoresed, and then electrotransferred to a nitrocellulose membrane. Membranes were incubated with anti-ICAM-1 and anti-VCAM-1 rabbit polyclonal antibodies (1:3,000 dilution in 5% BSA; R & D Systems, Minneapolis, MN) at room temperature for 1 h and then with rabbit polyclonal anti-GAPDH antibody (1:5,000 dilution; Cell Signaling Technology, Danvers, MA) for 1 h. Bound antibodies were detected with secondary antibodies conjugated to horseradish peroxidase (Cell Signaling Technology); then an ECL Plus chemiluminescence detection system reagent (Amersham Biosciences, Piscataway, NJ) was used to visualize the bands. Membrane-exposed X-ray films were scanned (Perfection 3200 scanner, Epson America, Long Beach, CA), and band density was quantified with densitometry software. Expression of VCAM-1 and ICAM-1 was normalized to GAPDH.

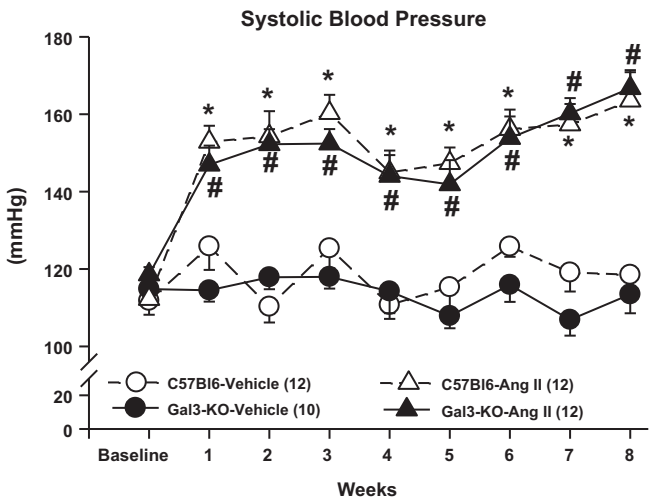


Fig. 1. Systolic blood pressure (SBP) in C57BL/6J and galectin 3 (Gal-3) knockout (KO) mice infused with angiotensin II (ANG II) or vehicle for 8 wk as measured by a computerized tail-cuff system. At baseline, SBP was similar among genotypes. ANG II increased blood pressure similarly in C57BL/6J and Gal-3 KO mice. Deletion of Gal-3 did not attenuate ANG II-induced hypertension in mice. *$P < 0.05$, C57BL/6J ANG II vs. C57BL/6J vehicle. #$P < 0.05$, Gal-3 KO ANG II vs. C57BL/6J vehicle.

Table 1. *Body, heart, and lung weight at 8 wk of follow-up*

| | Vehicle | | ANG II | |
|---|---|---|---|---|
| | C57BL/6J | Gal-3 KO | C57BL/6J | Gal-3 KO |
| Body wt, g | 30 ± 0.4 | 35 ± 0.8 | 30 ± 0.8 | 32 ± 0.9 |
| Heart wt, mg | 118 ± 11 | 124 ± 3 | 150 ± 5** | 165 ± 11*** |
| LV wt, mg | 96 ± 11 | 99 ± 3 | 127 ± 4** | 137 ± 11*** |
| Heart wt/TL, mg/cm | 64 ± 6 | 67 ± 2 | 82 ± 3** | 88 ± 6*** |
| LV wt/TL, mg/cm | 52 ± 6 | 53 ± 1 | 70 ± 2** | 73 ± 6*** |
| Lung wet wt/lung dry wt, mg/mg | 5 ± 0.5 | 4 ± 0.2 | 5 ± 0.6 | 4 ± 0.2 |

Values are means ± SE. ANG II, angiotensin II; Gal-3, galectin-3; KO, knockout; LV, left ventricle; TL, tibia length. **$P < 0.01$ vs. C57BL/6J vehicle. ***$P < 0.001$ vs. Gal-3 KO vehicle.

*Flow Cytometry*

Spleens were homogenized, and splenocytes were separated and harvested. Samples from each group were analyzed for total $CD4^+$ and $CD4^+/CD25^+/FOXP3^+$ ($T_{reg}$) lymphocytes by staining with FITC anti-rat CD4 antibody (Biolegend, San Diego, CA) and allophycocyanin-anti-rat CD25 antibody (eBioscience, San Diego, CA), as well as with their respective isotype-matched controls. Labeled splenocytes were fixed, permeabilized using eBioscience 1× permeabilization wash buffer, blocked with purified anti-mouse CD16/CD32 antibody (which blocks low-affinity Fcγ receptors), and stained with a species cross-reactive anti-FOXP3 antibody conjugated to phycoerythrin (BioLegend). Finally, cells were resuspended in 1% paraformaldehyde and stored at 4°C until analysis. Stained cells were acquired with a flow cytometer (model LSR, BD Biosciences). Fluorescence-event data were collected and analyzed using CellQuest Pro software (BD Biosciences) to determine the percentage of $CD4^+/CD25^+/FOXP3^+$ among total $CD4^+$ cells.

*Statistics*

Values are means ± SE. For all four groups, the Kruskal-Wallis test was followed by two-sample Wilcoxon tests. We compared differences between C57BL/6J ANG II and Gal-3 KO ANG II vs. C57BL/6J vehicle and C57BL/6J ANG II vs. Gal-3 KO ANG II. To determine significance, Hochberg's method was used on the two contrasts. $P < 0.05$ was considered statistically significant.

## RESULTS

*SBP and Body, Heart, and Lung Weight*

At baseline, SBP was similar among the four groups of animals (Fig. 1). In animals infused with vehicle, SBP remained at the baseline values for the duration of follow-up, with no difference between C57BL/6J and Gal-3 KO mice. Infusion of ANG II caused an increase in SBP that was not prevented by the absence of Gal-3 in Gal-3 KO mice. Within the group of normotensive mice, body weight, heart weight, and lung weight were similar, whereas the mice infused with ANG II displayed cardiac hypertrophy, which was similar in C57BL/6J and Gal-3 KO mice (Table 1).

*LV Remodeling and Function*

At baseline, IVST and PWT were similar among groups in both systole and diastole. Compared with vehicle control, ANG

Table 2. *Echocardiographic parameters at 8 wk of follow-up*

| | Vehicle | | ANG II | |
|---|---|---|---|---|
| | C57BL/6J | Gal-3 KO | C57BL/6J | Gal-3 KO |
| HR, beats/min | 682 ± 16 | 640 ± 10 | 664 ± 11 | 660 ± 10 |
| IVSTs, mm | 1.4 ± 0.1 | 1.4 ± 0.1 | 1.9 ± 0.1*** | 1.7 ± 0.1 |
| LV PWTs, mm | 1.3 ± 0.05 | 1.4 ± 0.04 | 2.1 ± 0.1*** | 1.9 ± 0.1** |
| LVDs, mm | 0.8 ± 0.1 | 0.9 ± 0.1 | 0.9 ± 0.1 | 0.9 ± 0.1 |
| LVAs, $mm^2$ | 0.8 ± 0.1 | 0.9 ± 0.2 | 1.7 ± 0.1*** | 1.0 ± 0.2## |
| IVSTd, mm | 0.9 ± 0.04 | 0.8 ± 0.02 | 1.2 ± 0.1*** | 1.1 ± 0.1* |
| LV PWTd, mm | 1.0 ± 0.04 | 1.0 ± 0.04 | 1.5 ± 0.1*** | 1.4 ± 0.1** |
| LVDd, mm | 2.4 ± 0.1 | 2.8 ± 0.1 | 2.2 ± 0.1# | 2.5 ± 0.2 |
| LVAd, $mm^2$ | 3.8 ± 0.1 | 4.6 ± 0.7 | 4.5 ± 0.3 | 4.2 ± 0.4 |

Values are means ± SE. s, Systole; d, diastole; HR, heart rate; IVST, interventricular septum thickness; PWT, posterior wall thickness; LVA, LV area; LVD, LV dimension. *$P < 0.05$ vs. Gal-3 KO vehicle. **$P < 0.01$ vs. Gal-3 KO vehicle. ***$P < 0.001$ vs. C57BL/6J vehicle. #$P = 0.05$ vs. Gal-3 KO ANG II. ##$P < 0.01$ vs. C57BL/6J ANG II.

II infusion significantly increased IVST. Specifically, in C57BL/6J mice, IVST increased from 1.4 ± 0.1 to 1.9 ± 0.1 mm in systole and from 0.9 ± 0.04 to 1.2 ± 0.1 mm in diastole. PWT was also significantly increased in systole and diastole in the C57BL/6J ANG II group, i.e., from 1.3 ± 0.05 to 2.1 ± 0.1 mm and from 1.0 ± 0.04 to 1.5 ± 0.1 mm, respectively; deletion of Gal-3 did not attenuate this increase (Table 2). In ANG II-infused C57BL/6J mice, systolic LV area was increased from 0.8 ± 0.1 to 1.7 ± 0.1 mm ($P < 0.05$ vs. control), but this effect was blunted in Gal-3 KO mice (1.0 ± 0.2 mm, $P < 0.05$ vs. C57BL/6J + ANG II; Fig. 2). As evaluated by EF (%) and SF (%), LV systolic function at baseline showed no differences among groups. However, after 8 wk of ANG II infusion, LV systolic function decreased in C57BL/6J mice from 84 ± 1 to 61 ± 3% and from 71 ± 0.3 to 57 ± 2% for EF and SF, respectively, but was well preserved in Gal-3 KO mice (77 ± 2 and 65 ± 2% for EF and SF, respectively; Fig. 2).

### *Myocardial Fibrosis, MCSA, and Capillary Density*

Normotensive mice showed similar myocardial collagen volume fraction (1.6 ± 0.5% for C57BL/6J and 2.4 ± 0.4% for Gal-3 KO mice). ANG II infusion caused significant myocardial fibrosis in C57BL/6J mice (9.3 ± 1.3%), but this effect was diminished in Gal-3 KO mice (3.4 ± 0.8%; Fig. 3, *A* and *B*).

Under normal conditions, MCSA was similar among the two mouse strains; C57BL/6J and Gal-3 KO animals chronically infused with ANG II showed significant myocyte hypertrophy (229 ± 12 and 200 ± 12 $\mu m^2$, respectively, $P = 0.03$) compared with the respective vehicle-infused mice (Fig. 3*C*). When infused with vehicle, capillary density was slightly, although not significantly, higher in Gal-3 KO than C57BL/6J mice. When infused with ANG II, Gal-3 KO mice also showed slightly higher capillary density than C57BL/6J mice, but the difference did not reach statistical significance (Fig. 3*D*).

### *Myocardial Macrophage Infiltration*

Few myocardial $CD68^+$ inflammatory cells were observed in C57BL/6J and Gal-3 KO mice infused with vehicle (34 ± 13 and 36 ± 7 cells/$mm^2$, respectively). However, infusion with ANG II significantly increased the numbers of infiltrating $CD68^+$ macrophages in the myocardium of C57BL/6J mice (118 ± 6 cells/$mm^2$), and this effect was almost completely abolished in Gal-3 KO mice (51 ± 10 cells/$mm^2$; Fig. 4).

### *Cardiac ICAM-1 and VCAM-1 Expression*

Western blot analysis showed similar amounts of cardiac ICAM-1 protein expression in normotensive mice (Fig. 5). However, ANG II infusion resulted in a significantly higher level of cardiac ICAM-1 expression in C57BL/6J, but not Gal-3 KO, mice. No differences were found in cardiac VCAM-1 expression among groups.

### *Plasma Cytokine Levels*

Circulating levels of IL-6 were similar in normotensive C57BL/6J and Gal-3 KO mice (4.5 ± 1.5 and 4.4 ± 0.4 pg/ml, respectively). However, infusion with ANG II resulted in a significant increase in plasma IL-6 levels in C57BL/6J (19 ± 5 pg/ml, $P = 0.028$), but not Gal-3 KO (2.6 ± 0.3 pg/ml), mice (Fig. 6). No differences were found in plasma levels of IL-10, MCP-1, or TNF-α among the groups. IL-12 and IFN-γ levels were below the assay detection limits.

### *Splenic T Lymphocytes*

No differences were found in numbers of splenic $CD4^+$ lymphocytes among the groups (Fig. 7*A*). Normotensive mice showed similar percentages of splenic $T_{reg}$ cells ($CD4^+/CD25^+/FOXP3^+$ lymphocytes). Interestingly, the percentages of $T_{reg}$ cells were unaffected by ANG II infusion in C57BL/6J mice but were increased significantly in Gal-3 KO mice (Fig. 7*B*).

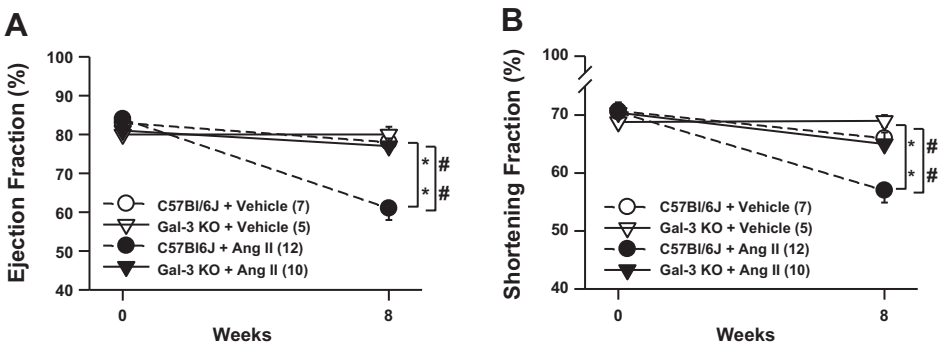


Fig. 2. Left ventricular (LV) ejection fraction (EF; *A*) and shortening fraction (SF, *B*) in mice infused with ANG II or vehicle. EF and SF were similar among groups at baseline. ANG II severely decreased EF and SF at 8 wk in C57BL/6J mice, but this decrease was attenuated in Gal-3 KO mice, suggesting that LV dysfunction was prevented by genetic deletion of Gal-3. *$P < 0.05$, C57BL/6J ANG II vs. C57BL/6J vehicle; ##$P < 0.05$, C57BL/6J ANG II vs. Gal-3 KO ANG II.

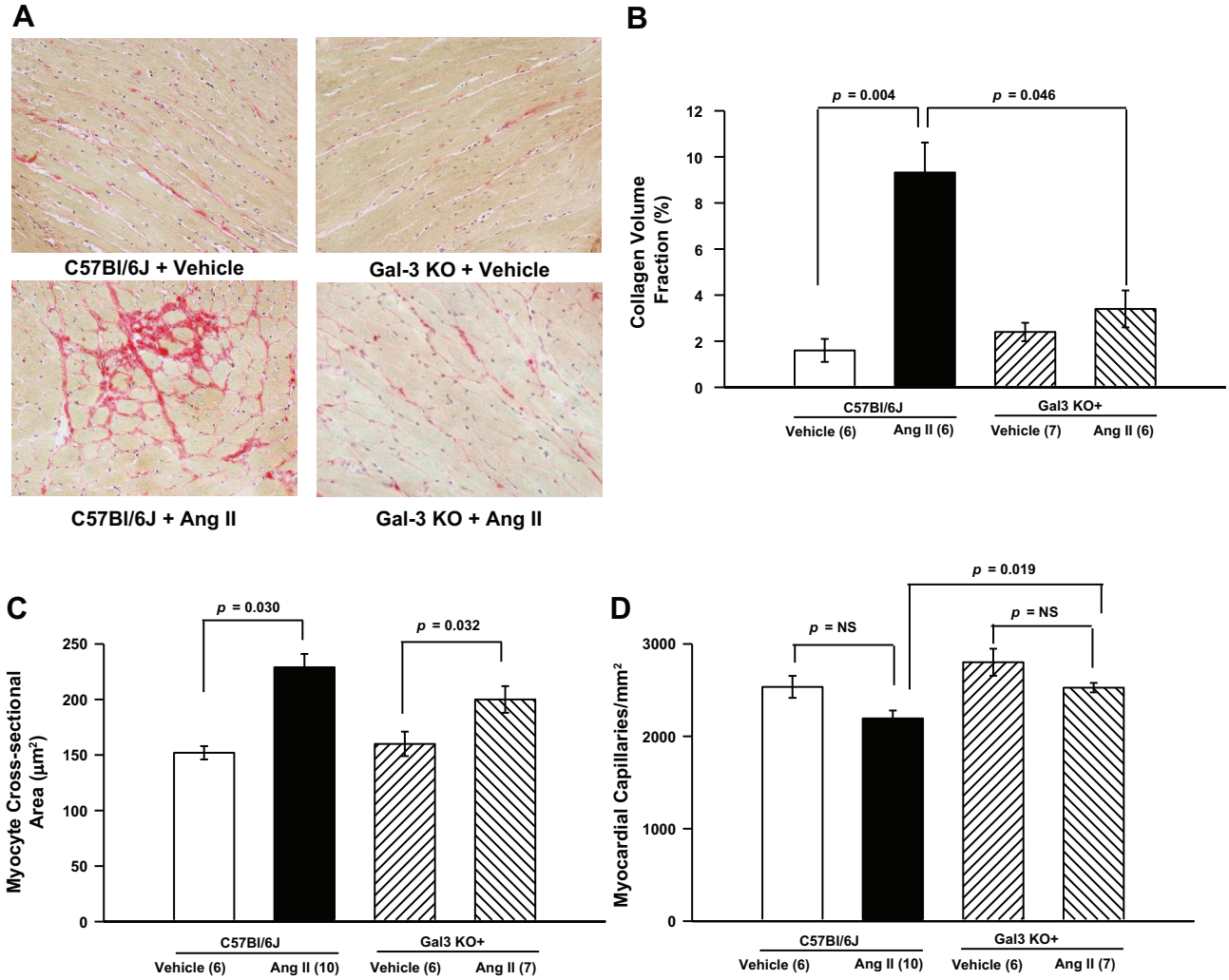


Fig. 3. *A* and *B*: representative PicroSirius red-stained images (magnification ×400) and myocardial collagen volume fraction quantification. ANG II induced significant myocardial fibrosis in C57BL/6J mice, but this effect was blunted in Gal-3 KO mice. *C*: myocyte cross-sectional area was significantly increased in C57BL/6J and Gal-3 KO mice infused with ANG II. *D*: capillary density was not different between mouse strains or treatment groups. NS, not significant.

## DISCUSSION

In ANG II-induced hypertension, we found that genetic Gal-3 deletion prevented myocardial macrophage infiltration and fibrosis. Gal-3 deficiency also preserved systolic function. Also, we provide evidence that this protective effect is accompanied by lower cardiac ICAM-1 expression and a decrease in plasma levels of IL-6, as well as an increase in the number of splenic $T_{reg}$ lymphocytes. Together, these results strongly suggest a modulatory role of Gal-3 in cardiac inflammation, fibrosis, and dysfunction induced by ANG II. Interestingly, genetic Gal-3 deletion affected neither hypertension nor myocardial hypertrophy. This observation suggests that myocardial hypertrophy is a direct mechanical consequence of hypertension and is not inflammation-dependent. Our results identify Gal-3 as a new and interesting therapeutic target for preventing the end-organ damage in ANG II-induced hypertension.

Previous studies showed that Gal-3 is involved in target organ damage (TOD) in human and experimental hypertension, as well as in nonhypertensive mice, independently of blood pressure and human cardiovascular disease (3, 11, 12, 26, 31, 47, 48). Here, to thoroughly delineate the role of Gal-3 in the pathogenesis of cardiac damage and dysfunction, we used a mouse model of ANG II-induced hypertension.

Chronic infusion with ANG II markedly increased blood pressure associated with myocardial hypertrophy in control C57BL/6J and Gal-3 KO mice. These findings are consistent with previous reports from Sharma et al. (42) and Yu et al. (51), who demonstrated that neither pharmacological inhibition nor genetic deletion of Gal-3 attenuated hypertension and cardiac hypertrophy. Thus our results clearly indicate that Gal-3 does not participate in development of ANG II-induced hypertension and cardiac hypertrophy.

Here, we found that Gal-3 deletion attenuated ANG II-induced cardiac fibrosis, confirming the data from our previous work demonstrating that exogenous Gal-3 infusion into a pericardial sac caused fibrosis (27). Moreover, ANG II is one of the most potent stimulators of aldosterone production, and this hormone mediates part of the cardiac profibrotic effect induced by ANG II infusion in mice (28). Interestingly, the profibrotic effect of aldosterone in the vasculature is mediated in part by Gal-3 (5, 48). Thus it is possible that the Gal-3 cardiac profibrotic effect represents an important downstream

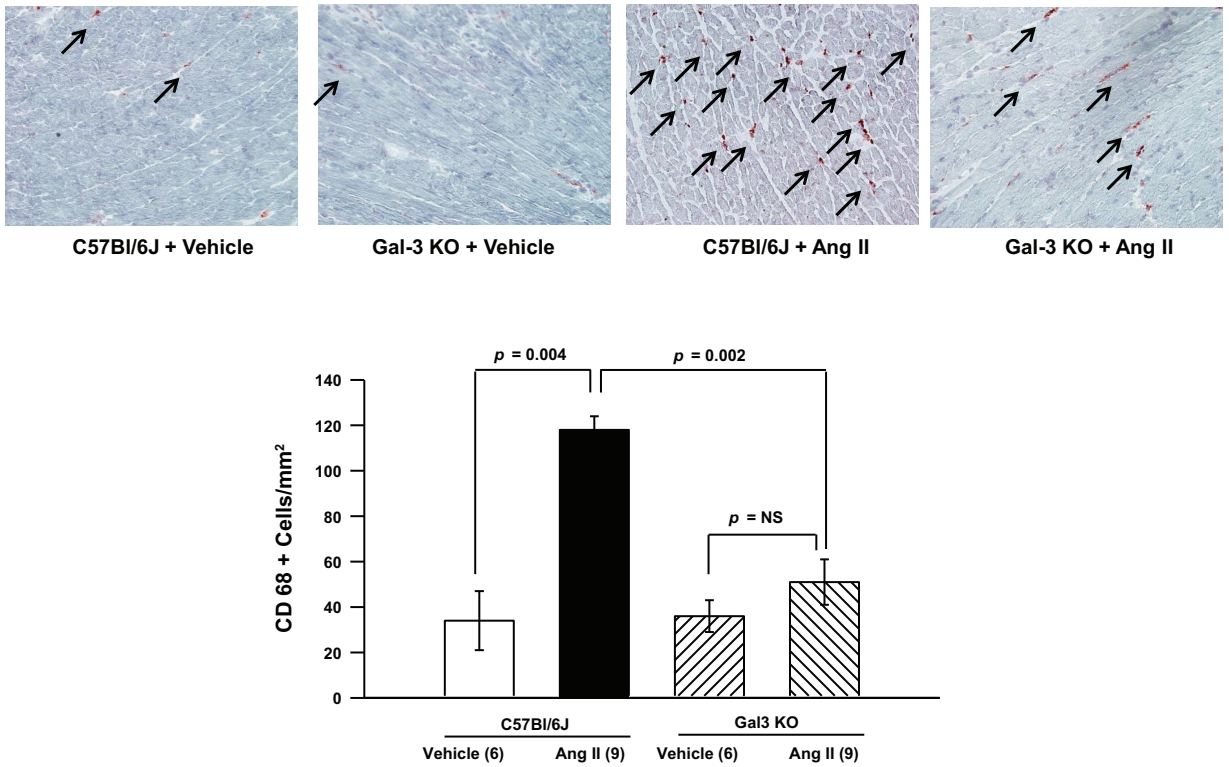


Fig. 4. Myocardial CD68$^+$ macrophage infiltration. *Top*: representative images (magnification ×400). Arrows indicate CD86$^+$ cells. *Bottom*: quantification. ANG II increased myocardial macrophage infiltration, but this increase was blunted in Gal-3 KO mice.

signaling event in the ANG II-aldosterone axis. Myocardial remodeling, inflammation, and fibrosis are considered hallmarks of hypertensive heart disease and cardiac dysfunction and indicators of poor prognosis (7, 27, 35, 37). Clinical evidence showed higher plasma Gal-3 concentrations in patients with acute and chronic heart failure. During the last few years, plasma levels of Gal-3 have been proposed as a strong prognostic marker of cardiac failure (9, 33), and Mayr et al. recently showed that these levels correlated with myocardial infarct size in patients (33). Recent studies show that age, hypertension, and renal function are the main determinants of Gal-3 concentrations in plasma (1). Therefore, we also analyzed the effect of Gal-3 deletion on cardiac remodeling and dysfunction. We observed LV systolic dysfunction in C57BL/6J mice infused with ANG II, as assessed by decreased EF and SF, and this LV dysfunction was completely prevented in Gal-3 KO mice.

The links among cardiac inflammation, subsequent fibrosis, and cardiac dysfunction are well established (16, 37, 42). However, Gal-3 participation in this process is incompletely understood. In a model of progressive renal fibrosis, Gal-3 was shown to be an important link between inflammation and fibrosis, such that Gal-3 secreted by macrophages activates fibroblasts to develop a profibrotic phenotype (19). Consistent with those observations, we found that both cardiac macrophage infiltration and fibrosis were markedly reduced in Gal-3 KO mice, which is consistent with our previous studies of pericardial infusion of Gal-3, showing increased cardiac fibrosis and dysfunction (26). Additionally, Yu et al. reported decreased cardiac fibrosis in Gal-3 KO mice with aortic banding (51). We previously reported that Gal-3 infusion into the pericardial sac of healthy Sprague-Dawley rats resulted in a higher number of infiltrating macrophages and fibrosis in the myocardium (26). Aside from affecting macrophage phenotype, Gal-3 may also affect the migration and tissue infiltration of these cells, and as demonstrated by Sano et al., Gal-3 could also contribute to macrophage phagocytosis through an intracellular mechanism (41). Endothelial cell adhesion molecules such as ICAM-1 and VCAM-1 play an important role in monocyte recruitment and migration from the circulation to the sites of injury (44). However, the influence of Gal-3 on cardiac adhesion molecule expression in ANG II-induced hypertension has not been examined. To investigate the mechanism by which Gal-3 deletion decreases macrophage infiltration, we evaluated myocardial ICAM-1 and VCAM-1 expression. Gal-3 deletion markedly attenuated ANG II-induced cardiac ICAM-1 expression. This observation agrees with the recent demonstration that Gal-3 can increase ICAM-1 expression in cultured endothelial cells (6). ANG II was shown to induce VCAM-1 expression in the rat vasculature after 6 days of infusion (46). However, we found no changes in cardiac VCAM-1 expression, which may result from the differences in protocol duration, species, or tissues studied relative to previous studies. Thus our study indicates that Gal-3 may partly mediate ANG II-induced monocyte recruitment by increasing ICAM-1 expression.

Cytokines are soluble factors produced by immune, endothelial, and other cell types and regulate many steps of immune responses, including those associated with hypertension (36, 52). However, the importance of Gal-3 as a regulator of inflammatory cytokines in TOD pathogenesis has yet to be elucidated. Here, we quantified the cytokines IL-6, IL-10,

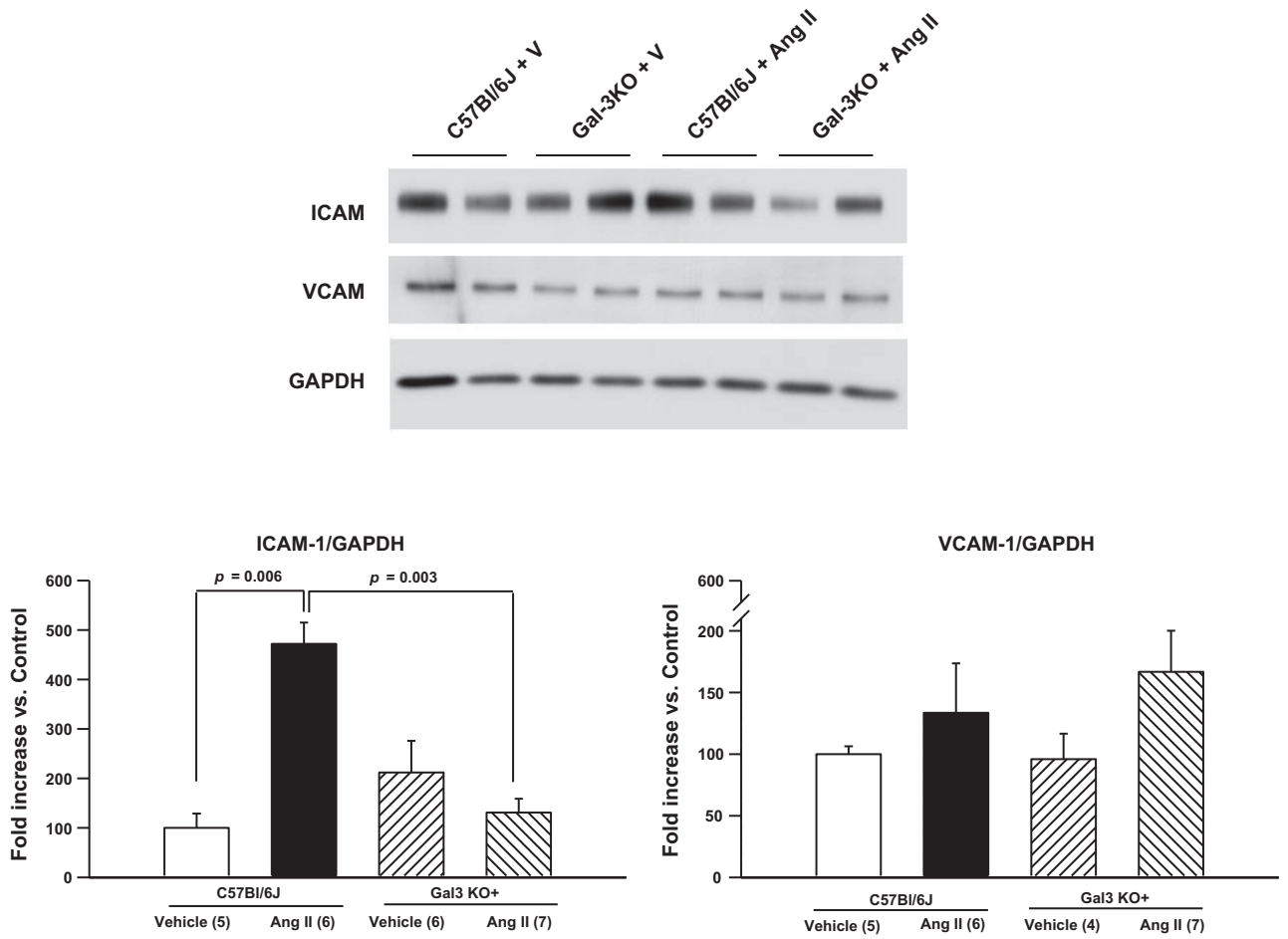


Fig. 5. Representative blots and quantitative analysis of ICAM-1 and VCAM-1 protein expression. ANG II infusion significantly increased myocardial ICAM-1 expression in C57BL/6J mice, but this effect was blunted in Gal-3 KO mice. No change in VCAM-1 expression was observed. V, vehicle.

IL-12, MCP-1, IFN-γ, and TNF-α, because the macrophages are among the main sources of these cytokines. After 8 wk of ANG II-induced hypertension, we found no change in circulating IL-10, IL-12, MCP-1, IFN-γ, or TNF-α between genotypes. However, one important finding of our investigation was that IL-6 was markedly enhanced in the plasma of C57BL/6J mice, but this increase was blunted in Gal-3 KO mice. IL-6 participates in the development of hypertensive TOD development by promoting inflammation and fibrosis in the heart and kidney (24, 34, 52). We recently demonstrated that genetic deletion of IL-6 attenuated ANG II-high salt-induced hypertension and cardiac dysfunction (15). Thus our results strongly suggest that some of the detrimental effects of Gal-3 on the heart may be mediated by IL-6 and by macrophage infiltration.

Gal-3 has been detected in T cell subsets, including $T_{reg}$ ($CD4^+/CD25^+/FOXP3^+$) cells (8). Therefore, we studied whether genetic deletion of Gal-3 might prevent TOD in part by modifying the T cell profile. We found no significant changes in splenic $CD4^+$ lymphocytes between the two mouse strains infused with vehicle or ANG II; however, Gal-3 deletion was associated with an interesting effect on $T_{reg}$ cells: ANG II had no effect on $T_{reg}$ cells in C57BL/6J mice but nearly doubled the number of splenic $T_{reg}$ cells in Gal-3 KO mice. This finding is consistent with previous reports showing a higher number of $T_{reg}$ cells in Gal-3 KO mice (13, 21). Moreover, $T_{reg}$ cell transfer has been shown to attenuate ANG II-induced increases in IL-6 and perivascular macrophage infiltration (2, 32). Adoptive transfer of $T_{reg}$ cells was shown to ameliorate ANG II-induced cardiac damage (23) not only by marked reduction in $CD4^+$, $CD8^+$, and $CD69^+$ cells, but also by macrophage infiltration. Thus one could speculate that Gal-3 may act as an endogenous inhibitor of $T_{reg}$ cells, resulting in unopposed immune/inflammatory cells and, thereby, contributing to tissue damage during ANG II-induced hypertension.

In summary, genetic deletion of Gal-3 prevents TOD and LV systolic dysfunction without altering blood pressure or LV hypertrophy in ANG II-induced hypertension. Our results indicate that the detrimental effects of ANG II could be, in part, mediated by Gal-3, which decreases the percentage of $T_{reg}$ cells and increases the percentage of proinflammatory adhesion molecules and cytokines, the proportion of myocardial macrophages infiltrating the myocardium, and fibrosis.

### *Study Limitation*

Although inflammatory cells and fibroblasts are the main source of Gal-3, it remains unknown whether the local source or systemic production of Gal-3 contributes most to the TOD in ANG II-dependent hypertension.

The present data show lower proportions of infiltrating cardiac macrophages in Gal-3 KO mice, indicating that macrophages may be one of the cell types responsible for the protective effect. The cell type or organ that is the source of Gal-3 contributing to cardiac damage in ANG II-dependent hypertension remains to be identified. Further studies are needed to investigate the underlying mechanism by which Gal-3 regulates $T_{reg}$ cells. Our results were obtained solely from a mouse model of hypertension induced by chronic infusion of ANG II, and the complexity and multiplicity of mechanisms involved in human cardiac remodeling and dysfunction in hypertension were not addressed. Thus, further investigations are needed to fully support the translational relevance of the present study.

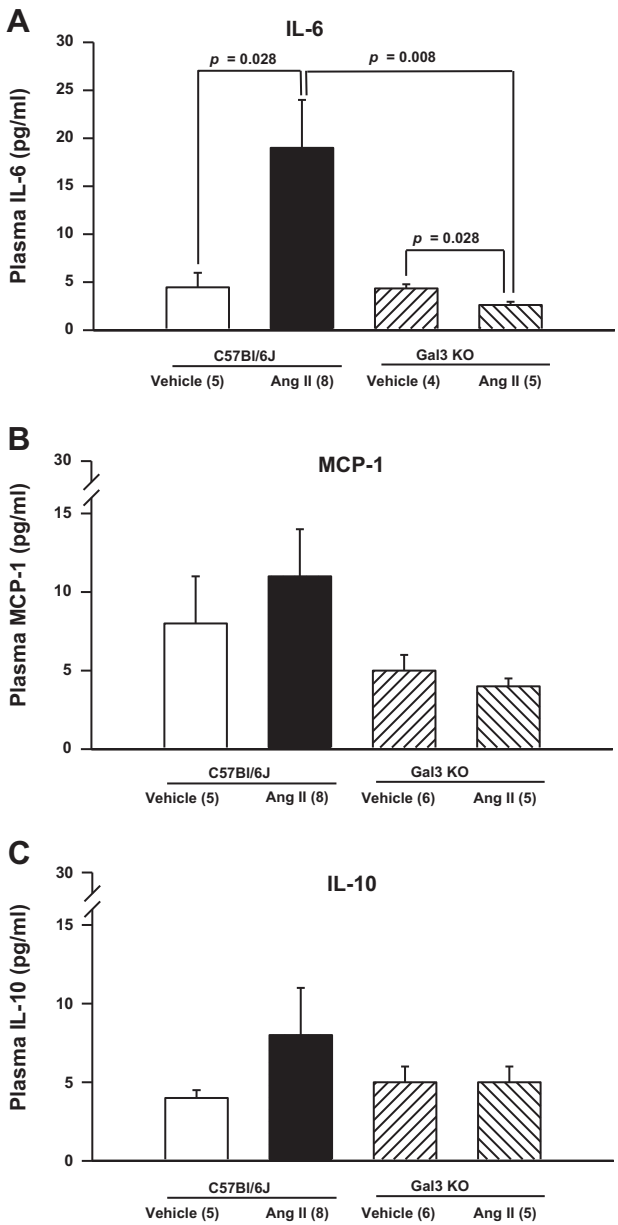


Fig. 6. Quantitative analysis of plasma levels of IL-6 (*A*), monocyte chemoattractant protein-1 (MCP-1; *B*), and IL-10 (*C*). ANG II increased plasma concentration of IL-6, but this effect was blunted in Gal-3 KO mice. Changes in circulating levels of IL-10 or MCP-1 did not reach statistical significance.

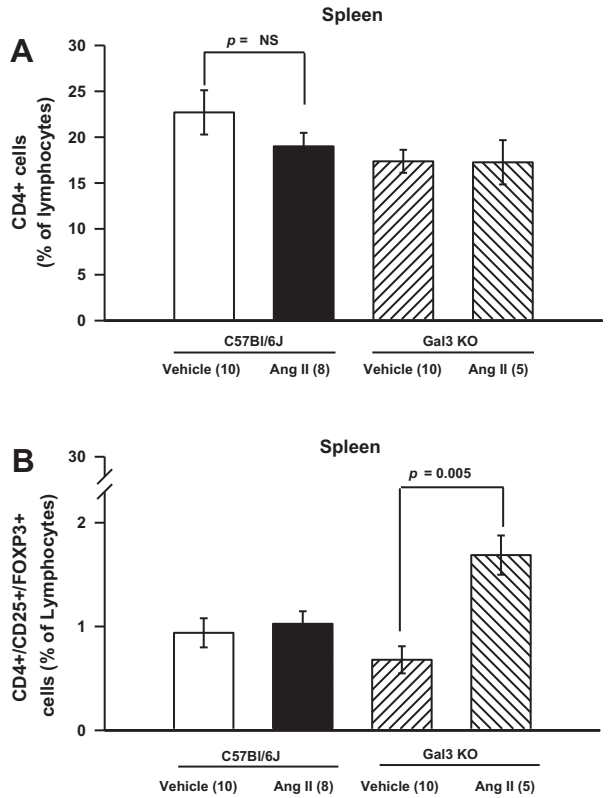


Fig. 7. *A*: total $CD4^+$ helper T cells. *B*: $CD4^+$ $Foxp3^+$ $T_{reg}$ cells. Spleen $CD4^+$ and $CD4^+/CD25^+/FOXP3^+$ ($T_{reg}$) lymphocytes. ANG II had no effect on percentage of $CD4^+$ and $T_{reg}$ lymphocytes. However, percentage of splenic $T_{reg}$ cells was significantly increased in ANG II-infused Gal-3 KO mice.

## *Perspectives*

Development of cardiac myocyte hypertrophy, inflammation, and fibrosis is a hallmark of cardiac remodeling and dysfunction. Progressive cardiac remodeling is the main predictor of heart failure development. An emerging body of evidence suggests that the serum level of Gal-3 is an even more powerful predictor of mortality than the well-known predictor pro-B-type natriuretic peptide in patients with decompensated heart failure (9). Our study suggests that Gal-3 is not only a marker, but also a mediator, of cardiac inflammation, fibrosis, and dysfunction. Thus, antagonistic strategies targeting Gal-3 may be a novel therapeutic approach in providing the cardiac protection in hypertension and heart failure.

## ACKNOWLEDGMENTS

The technical support of D. Smolarek, G. Gürocak, and C. Polomski is greatly appreciated.

## GRANTS

Research reported in this publication was supported by National Heart, Lung, and Blood Institute Grant HL-028982 (O. A. Carretero), Henry Ford Health System institutional funds (N. E. Rhaleb), University of Buenos Aires UBACyT Grant 20020130200172BA (G. E. González), and National Agency for Science and Technology Promotion PICT 2014-2320 (G. E. González).

## DISCLAIMERS

The content is solely the responsibility of the authors and does not necessarily represent the official views of the National Institutes of Health.

## DISCLOSURES

No conflicts of interest, financial or otherwise, are declared by the authors.

## AUTHOR CONTRIBUTIONS

G.E.G., N.-E.R., and O.A.C. developed the concept and designed the research; G.E.G., N.-E.R., P.N., T.-D.L., P.L., X.D., Y.-H.L., and X.-P.Y. performed the experiments; G.E.G., N.-E.R., P.N., X.-P.Y., and O.A.C. analyzed the data; G.E.G., N.-E.R., E.L.P., X.D., Y.-H.L., X.-P.Y., and O.A.C. interpreted the results of the experiments; G.E.G., N.-E.R., M.A.D., B.J., and O.A.C. prepared the figures; G.E.G., N.-E.R., M.A.D., and O.A.C. drafted the manuscript; G.E.G., N.-E.R., M.A.D., P.N., T.-D.L., P.L., X.D., B.J., Y.-H.L., X.-P.Y., and O.A.C. edited and revised the manuscript; G.E.G., N.-E.R., M.A.D., P.N., T.-D.L., E.L.P., P.L., X.D., B.J., Y.-H.L., X.-P.Y., and O.A.C. approved the final version of the manuscript.

## REFERENCES


1. **Arangalage D, Nguyen V, Robert T, Melissopoulou M, Mathieu T, Estellat C, Codogno I, Huart V, Duval X, Cimadevilla C, Vahanian A, Dehoux M, Messika-Zeitoun D.** Determinants and prognostic value of galectin-3 in patients with aortic valve stenosis. *Heart* 102: 862–868, 2016.
2. **Barhoumi T, Kasal DA, Li MW, Shbat L, Laurant P, Neves MF, Paradis P, Schiffrin EL.** T regulatory lymphocytes prevent angiotensin II-induced hypertension and vascular injury. *Hypertension* 57: 469–476, 2011.
3. **Bozcali E, Polat V, Aciksari G, Opan S, Bayrak İH, Paker N, Karakaya O.** Serum concentrations of galectin-3 in patients with cardiac syndrome X. *Atherosclerosis* 237: 259–263, 2014.
4. **Brands MW, Banes-Berceli AK, Inscho EW, Al-Azawi H, Allen AJ, Labazi H.** Interleukin 6 knockout prevents angiotensin II hypertension: role of renal vasoconstriction and Janus kinase 2/signal transducer and activator of transcription 3 activation. *Hypertension* 56: 879–884, 2010.
5. **Calvier L, Miana M, Reboul P, Cachofeiro V, Martinez-Martinez E, de Boer RA, Poirier F, Lacolley P, Zannad F, Rossignol P, Lopez-Andres N.** Galectin-3 mediates aldosterone-induced vascular fibrosis. *Arterioscler Thromb Vasc Biol* 33: 67–75, 2013.
6. **Chen C, Duckworth CA, Zhao Q, Pritchard DM, Rhodes JM, Yu LG.** Increased circulation of galectin-3 in cancer induces secretion of metastasis-promoting cytokines from blood vascular endothelium. *Clin Cancer Res* 19: 1693–1704, 2013.
7. **Cingolani OH, Yang XP, Liu YH, Villanueva M, Rhaleb NE, Carretero OA.** Reduction of cardiac fibrosis decreases systolic performance without affecting diastolic function in hypertensive rats. *Hypertension* 43: 1067–1073, 2004.
8. **Cummings RD, Liu FT.** Galectins. In: *Essentials of Glycobiology*, edited by Varki A, Cummings RD, Esko JD, Freeze HH, Stanley P, Bertozzi CR, Hart GW, Etzler ME. Cold Spring Harbor, NY: Cold Spring Harbor Laboratory, 2009, p. 475–488.
9. **de Boer RA, Lok DJ, Jaarsma T, van der Meer P, Voors AA, Hillege HL, van Veldhuisen DJ.** Predictive value of plasma galectin-3 levels in heart failure with reduced and preserved ejection fraction. *Ann Med* 43: 60–68, 2011.
10. **de Boer RA, Yu L, van Veldhuisen DJ.** Galectin-3 in cardiac remodeling and heart failure. *Curr Heart Fail Rep* 7: 1–8, 2010.
11. **Falcone C, Lucibello S, Mazzucchelli I, Bozzini S, D'Angelo A, Schirinzi S, Totaro R, Falcone R, Bondesan M, Pelissero G.** Galectin-3 plasma levels and coronary artery disease: a new possible biomarker of acute coronary syndrome. *Int J Immunopathol Pharmacol* 24: 905–913, 2011.
12. **Fenster BE, Lasalvia L, Schroeder JD, Smyser J, Silveira LJ, Buckner JK, Brown KK.** Galectin-3 levels are associated with right ventricular functional and morphologic changes in pulmonary arterial hypertension. *Heart Vessels* 31: 939–946, 2016.
13. **Fermino ML, Dias FC, Lopes CD, Souza MA, Cruz AK, Liu FT, Chammas R, Roque-Barreira MC, Rabinovich GA, Bernardes ES.** Galectin-3 negatively regulates the frequency and function of $CD4^+CD25^+Foxp3^+$ regulatory T cells and influences the course of *Leishmania major* infection. *Eur J Immunol* 43: 1806–1817, 2013.
14. **Gonzalez GE, Cassaglia P, Noli Truant S, Fernandez MM, Wilensky L, Volberg V, Malchiodi EL, Morales C, Gelpi RJ.** Galectin-3 is essential for early wound healing and ventricular remodeling after myocardial infarction in mice. *Int J Cardiol* 176: 1423–1425, 2014.
15. **Gonzalez GE, Rhaleb NE, D'Ambrosio MA, Nakagawa P, Liu Y, Leung P, Dai X, Yang XP, Peterson EL, Carretero OA.** Deletion of interleukin-6 prevents cardiac inflammation, fibrosis and dysfunction without affecting blood pressure in angiotensin II-high salt-induced hypertension. *J Hypertens* 33: 144–152, 2015.
16. **Gonzalez GE, Rhaleb NE, Nakagawa P, Liao TD, Liu Y, Leung P, Dai X, Yang XP, Carretero OA.** *N*-acetyl-seryl-aspartyl-lysyl-proline reduces cardiac collagen cross-linking and inflammation in angiotensin II-induced hypertensive rats. *Clin Sci (Lond)* 126: 85–94, 2014.
17. **Greene AS, Rieder MJ.** Measurement of vascular density. *Methods Mol Med* 51: 489–496, 2001.
18. **Hansen-Smith FM, Watson L, Lu DY, Goldstein I.** *Griffonia simplicifolia* I: fluorescent tracer for microcirculatory vessels in nonperfused thin muscles and sectioned muscle. *Microvasc Res* 36: 199–215, 1988.
19. **Henderson NC, MacKinnon AC, Farnworth SL, Kipari T, Haslett C, Iredale JP, Liu FT, Hughes J, Sethi T.** Galectin-3 expression and secretion links macrophages to the promotion of renal fibrosis. *Am J Pathol* 172: 288–298, 2008.
20. **Hsu DK, Yang RY, Pan Z, Yu L, Salomon DR, Fung-Leung WP, Liu FT.** Targeted disruption of the galectin-3 gene results in attenuated peritoneal inflammatory responses. *Am J Pathol* 156: 1073–1083, 2000.
21. **Jiang HR, Al RZ, Mensah-Brown E, Shahin A, Xu D, Goodyear CS, Fukada SY, Liu FT, Liew FY, Lukic ML.** Galectin-3 deficiency reduces the severity of experimental autoimmune encephalomyelitis. *J Immunol* 182: 1167–1173, 2009.
22. **Kim H, Lee J, Hyun JW, Park JW, Joo HG, Shin T.** Expression and immunohistochemical localization of galectin-3 in various mouse tissues. *Cell Biol Int* 31: 655–662, 2007.
23. **Kvakan H, Kleinewietfeld M, Qadri F, Park JK, Fischer R, Schwarz I, Rahn HP, Plehm R, Wellner M, Elitok S, Gratze P, Dechend R, Luft FC, Muller DN.** Regulatory T cells ameliorate angiotensin II-induced cardiac damage. *Circulation* 119: 2904–2912, 2009.
24. **Lee DL, Sturgis LC, Labazi H, Osborne JB Jr, Fleming C, Pollock JS, Manhiani M, Imig JD, Brands MW.** Angiotensin II hypertension is attenuated in interleukin-6 knockout mice. *Am J Physiol Heart Circ Physiol* 290: H935–H940, 2006.
25. **Liao TD, Yang XP, D'Ambrosio M, Zhang Y, Rhaleb NE, Carretero OA.** *N*-acetyl-seryl-aspartyl-lysyl-proline attenuates renal injury and dysfunction in hypertensive rats with reduced renal mass: Council for High Blood Pressure Research. *Hypertension* 55: 459–467, 2010.
26. **Liu YH, D'Ambrosio M, Liao TD, Peng H, Rhaleb NE, Sharma U, Andre S, Gabius HJ, Carretero OA.** *N*-acetyl-seryl-aspartyl-lysyl-proline prevents cardiac remodeling and dysfunction induced by galectin-3, a mammalian adhesion/growth-regulatory lectin. *Am J Physiol Heart Circ Physiol* 296: H404–H412, 2009.
27. **Liu YH, D'Ambrosio MA, Liao TD, Peng HM, Rhaleb NE, Sharma U, Carretero OA.** Ac-SDKP prevents cardiac fibrosis and dysfunction induced by galectin-3: role of TGF-β/Smad3 signaling pathway (Abstract). *FASEB J* 23: 362, 2009.
28. **Liu YH, Xu J, Yang XP, Yang F, Shesely E, Carretero OA.** Effect of ACE inhibitors and angiotensin II type 1 receptor antagonists on endothelial NO synthase knockout mice with heart failure. *Hypertension* 39: 375–381, 2002.
29. **Liu YH, Yang XP, Sharov VG, Nass O, Sabbah HN, Peterson E, Carretero OA.** Effects of angiotensin-converting enzyme inhibitors and angiotensin II type 1 receptor antagonists in rats with heart failure. Role of kinins and angiotensin II type 2 receptors. *J Clin Invest* 99: 1926–1935, 1997.
30. **Lok DJ, van der Meer P, de la Porte PW, Lipsic E, Van Wijngaarden J, Hillege HL, van Veldhuisen DJ.** Prognostic value of galectin-3, a novel marker of fibrosis, in patients with chronic heart failure: data from the DEAL-HF study. *Clin Res Cardiol* 99: 323–328, 2010.
31. **Martínez-Martínez E, Calvier L, Fernández-Celis A, Rousseau E, Jurado-López R, Rossoni LV, Jaisser F, Zannad F, Rossignol P, Cachofeiro V, López-Andrés N.** Galectin-3 blockade inhibits cardiac inflammation and fibrosis in experimental hyperaldosteronism and hypertension. *Hypertension* 66: 767–775, 2015.
32. **Matrougui K, Zakaria AE, Kassan M, Choi S, Nair D, Gonzalez-Villalobos RA, Chentoufi AA, Kadowitz P, Belmadani S, Partyka M.**

Natural regulatory T cells control coronary arteriolar endothelial dysfunction in hypertensive mice. *Am J Pathol* 178: 434–441, 2011.
33. **Mayr A, Klug G, Mair J, Streil K, Harrasser B, Feistritzer HJ, Jaschke W, Schocke M, Pachinger O, Metzler B.** Galectin-3: relation to infarct scar and left ventricular function after myocardial infarction. *Int J Cardiol* 163: 335–337, 2013.
34. **Melendez GC, McLarty JL, Levick SP, Du Y, Janicki JS, Brower GL.** Interleukin 6 mediates myocardial fibrosis, concentric hypertrophy, and diastolic dysfunction in rats. *Hypertension* 56: 225–231, 2010.
35. **Nakagawa P, Liu Y, Liao TD, Chen X, Gonzalez GE, Bobbitt KR, Smolarek D, Peterson EL, Kedl R, Yang XP, Rhaleb NE, Carretero OA.** Treatment with *N*-acetyl-seryl-aspartyl-lysyl-proline prevents experimental autoimmune myocarditis in rats. *Am J Physiol Heart Circ Physiol* 303: H1114–H1127, 2012.
36. **Peeters AC, Netea MG, Janssen MC, Kullberg BJ, van der Meer JW, Thien T.** Pro-inflammatory cytokines in patients with essential hypertension. *Eur J Clin Invest* 31: 31–36, 2001.
37. **Peng H, Yang XP, Carretero OA, Nakagawa P, D'Ambrosio M, Leung P, Xu J, Peterson EL, Gonzalez GE, Harding P, Rhaleb NE.** Angiotensin II-induced dilated cardiomyopathy in Balb/c but not C57BL/6J mice. *Exp Physiol* 96: 756–764, 2011.
38. **Rabinovich GA, Toscano MA.** Turning "sweet" on immunity: galectin-glycan interactions in immune tolerance and inflammation. *Nat Rev Immunol* 9: 338–352, 2009.
39. **Rakusan K.** Changes in the myocardial oxygen tension caused by changes in several oxygen determinants, with special consideration of the diffusion distance. In: *Oxygen in the Heart Muscle*. Springfield, IL: Thomas, 1971, p. 66–71.
40. **Sahn DJ, DeMaria A, Kisslo J, Weyman A.** Recommendations regarding quantitation in M-mode echocardiography: results of a survey of echocardiographic measurements. *Circulation* 58: 1072–1083, 1978.
41. **Sano H, Hsu DK, Apgar JR, Yu L, Sharma BB, Kuwabara I, Izui S, Liu FT.** Critical role of galectin-3 in phagocytosis by macrophages. *J Clin Invest* 112: 389–397, 2003.
42. **Sharma U, Rhaleb NE, Pokharel S, Harding P, Rasoul S, Peng H, Carretero OA.** Novel anti-inflammatory mechanisms of *N*-acetyl-Ser-Asp-Lys-Pro in hypertension-induced target organ damage. *Am J Physiol Heart Circ Physiol* 294: H1226–H1232, 2008.
43. **Sharma UC, Pokharel S, van Brakel TJ, van Berlo JH, Cleutjens JP, Schroen B, Andr S, Crijns HJ, Gabius HJ, Maessen J, Pinto YM.** Galectin-3 marks activated macrophages in failure-prone hypertrophied hearts and contributes to cardiac dysfunction. *Circulation* 110: 3121–3128, 2004.
44. **Shi C, Pamer EG.** Monocyte recruitment during infection and inflammation. *Nat Rev Immunol* 11: 762–774, 2011.
45. **Sun Y, Carretero OA, Xu J, Rhaleb NE, Yang JJ, Pagano PJ, Yang XP.** Deletion of inducible nitric oxide synthase provides cardioprotection in mice with 2-kidney, 1-clip hypertension. *Hypertension* 53: 49–56, 2009.
46. **Tummala PE, Chen XL, Sundell CL, Laursen JB, Hammes CP, Alexander RW, Harrison DG, Medford RM.** Angiotensin II induces vascular cell adhesion molecule expression in rat vasculature. A potential link between the renin-angiotensin system and atherosclerosis. *Circulation* 100: 1223–1229, 1999.
47. **Vergaro G, Del Franco A, Giannoni A, Prontera C, Ripoli A, Barison A, Masci PG, Aquaro GD, Cohen Solal A, Padeletti L, Passino C, Emdin M.** Galectin-3 and myocardial fibrosis in nonischemic dilated cardiomyopathy. *Int J Cardiol* 184: 96–100, 2015.
48. **Vergaro G, Prud'homme M, Fazal L, Merval R, Passino C, Emdin M, Samuel JL, Cohen Solal A, Delcayre C.** Inhibition of galectin-3 pathway prevents isoproterenol-induced left ventricular dysfunction and fibrosis in mice. *Hypertension* 67: 606–612, 2016.
49. **Wang D, Carretero OA, Yang XY, Rhaleb NE, Liu YH, Liao TD, Yang XP.** *N*-acetyl-seryl-aspartyl-lysyl-proline stimulates angiogenesis in vitro and in vivo. *Am J Physiol Heart Circ Physiol* 287: H2099–H2105, 2004.
50. **Yang XP, Liu YH, Rhaleb NE, Kurihara N, Kim HE, Carretero OA.** Echocardiographic assessment of cardiac function in conscious and anesthetized mice. *Am J Physiol Heart Circ Physiol* 277: H1967–H1974, 1999.
51. **Yu L, Ruifrok WP, Meissner M, Bos EM, van Goor H, Sanjabi B, van der Harst P, Pitt B, Goldstein IJ, Koerts JA, van Veldhuisen DJ, Bank RA, van Gilst WH, Sillje HH, de Boer RA.** Genetic and pharmacological inhibition of galectin-3 prevents cardiac remodeling by interfering with myocardial fibrogenesis. *Circ Heart Fail* 6: 107–117, 2013.
52. **Zhang W, Wang W, Yu H, Zhang Y, Dai Y, Ning C, Tao L, Sun H, Kellems RE, Blackburn MR, Xia Y.** Interleukin 6 underlies angiotensin II-induced hypertension and chronic renal damage. *Hypertension* 59: 136–144, 2012.